Visualization of heaving aerofoil wakes including the effect of a jet flap

By C. J. WOOD and S. F. A. KIRMANI†

Department of Engineering Science, University of Oxford

Theoretical solutions exist for the flow about aerofoils in various modes of unsteady motion. This is also true for aerofoils whose lift is augmented by a jet flap. A common feature of these theories is the assumption of small amplitude displacements from the mean path and the generation of a continuous vortex sheet wake. However, in practice when the motion is oscillatory and of finite amplitude, an alternating trail of individual vortices is often found. The present visual investigation includes the measurement of some vortex street parameters associated with heaving aerofoils. The results are compared with those of conventional thin aerofoil theory in order to assess the significance of this departure from the conventional small displacement flow model.

1. Introduction

The motive for the present investigation was the desire to gain an improved understanding of the mechanism which relates two-dimensional wake vortex trails to the body flows which cause them. The controlled generation of vortex trails by a heaving aerofoil was chosen because in this case the existence of a theoretical solution (Robinson & Laurmann 1956) makes possible an illuminating assessment of the vortex shedding mechanism in the light of the theoretical variations in circulation.

When considering the application of these theoretical results, however, a major problem arises at once. This is the striking difference between the actual wake flow with its alternate trail of individual vortices and the theoretical wake which is represented simply by a continuous distribution of vorticity along the mean aerofoil path. Consequently there is almost certainly some error involved in the application of these theoretical results in vortex shedding situations.

In view of this difficulty, the present investigation serves a dual purpose. First, if the theoretical solution is found to be significant in relation to the generation of vortices, then its value may be established in areas where it has previously been neglected. These areas include the problems of plate vibration and even acoustic resonance caused by vortex shedding (Toebes & Eagleson 1961; Parker 1966 *a*, *b*, 1967 *a*, *b*). Alternatively, if the theory is seriously in error in the presence of a vortex trail, then the present experiment may emphasize more clearly the limits of validity of the small displacement assumption.

† Present address: British Aircraft Corporation, Weybridge, Surrey.

The work was extended to include the jet flap case for a more specific reason. In a theoretical treatment of heaving jet flap aerofoils, Spence (1965) discovered a particular combination of jet strength and oscillation frequency for which no solution was possible. The investigation described in part 2 of this paper was initiated with the object of discovering whether or not the theoretical failing case represents a real flow phenomenon.

2. Flow visualization

The equipment and the methods used in these experiments have been described in some detail in earlier papers (Wood 1967, 1968). Briefly, the aerofoil was mounted under a trolley and towed at constant velocity in a tank of still water. A suspension of 0·2 mm diameter neutrally buoyant polystyrene beads in the water was illuminated in a horizontal plane by 20–30 mm thick parallel beams of light from mercury vapour lamps. The 100 Hz flashing of these lamps provided a convenient time marker when the flow was photographed by a stationary camera, viewing vertically from beneath the glass bottom of the tank.

The oscillatory motion of the aerofoil was arranged by mounting it on a swinging sub-frame under the moving trolley. The frame was suspended on four spring steel strips and was capable of moving horizontally and without rotation in a direction transverse to the mean motion. It was driven sinusoidally by two crank wheels on a common horizontal shaft. Nylon rollers on the crank wheel were retained in spring loaded contact with vertical thrust posts on the swinging frame. The eccentricity of these rollers could be varied from 0 to 30 mm by repositioning the secondary eccentric mounting plates which carried them. This controlled the amplitude of the heaving motion.

The oscillatory system was driven at an infinitely variable speed by an electric pistol drill with a specially constructed feedback speed control. To tow the trolley, a cable and drum system was geared to a constant speed induction motor. Both the shaking frequency and the trolley speed were constant to within $\pm 2\%$ and their mean values for any test were recorded by stopwatch. With an aerofoil chord c of 153 mm and a trolley speed U of 0·093 m/s the Reynolds number was $1·25 \times 10^4$ and the Strouhal number $S\,(=fc/U)$ could be varied from 0·7 to 2·7.

The aerofoil model was designed initially for the jet flap experiments. The nose was elliptical in section with major and minor semi-axes 63·5 mm and 12·7 mm and was machined from perspex in two halves. These were clamped together round a tubular brass spine of 16 mm bore which formed both the support and also the distribution manifold for the jet flow. The rear surfaces formed a straight taper, extending symmetrical tangents from the ellipse to give a trailing edge thickness of 2·5 mm at the stated chord length. Two brass plates formed this portion and at the trailing edge their internal surfaces were bevelled to form a parallel slit 2·06 mm wide. The model was used without modification for the plain aerofoil experiments.

3. Results: Heaving aerofoil with no jet

The vortex trail

Figure 1, plate 1, shows a typical flow at $S = 1.62$, $y_0/c = 0.067$. The frequency of vortex shedding is determined by the oscillation frequency so that in each half cycle a vortex leaves the trailing edge and is swept into the wake. A careful examination of figure 1 shows that this new vortex grows as the aerofoil moves inwards from its peak displacement. During the growth phase the vortex is drawn outwards from the aerofoil and it is shed without crossing the mean path
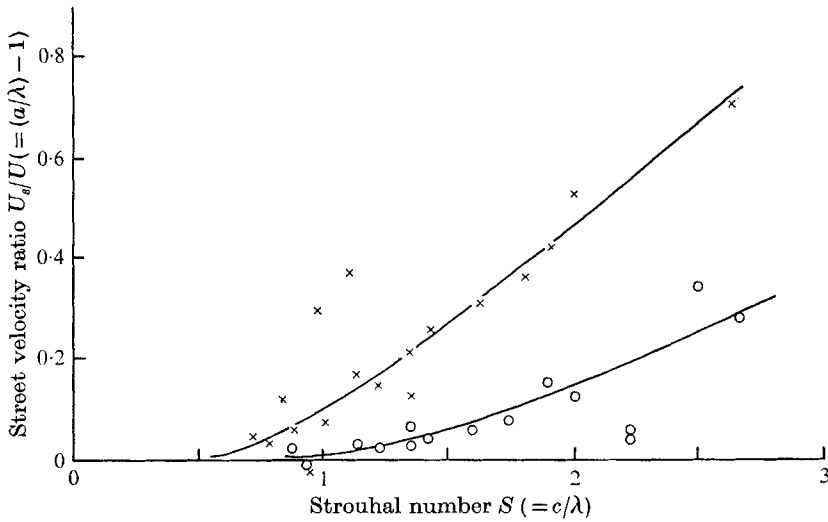

FIGURE 2. Variation of longitudinal vortex spacing a with frequency.
$\times$, $y_0/c = 0.067$; $\bigcirc$, $y_0/c = 0.033$.

centreline. Thus the sense of rotation in the vortex trail is opposite to that normally associated with the classical von Kármán vortex street. The momentum of this flow pattern is in the thrust sense and the mutually induced longitudinal velocity U_s of the vortices is directed away from the aerofoil (Michelson 1963).

This street velocity is related directly to the frequency f and to the longitudinal spacing a by the equation

$$U + U_s = fa$$

or, in terms of the wavelength $\lambda\ (= U/f)$

$$U_s/U = a/\lambda - 1.$$

This velocity ratio is plotted in figure 2 for two values of the oscillation amplitude y_0/c.

The variation in magnitude shows that the strength of the vortex trail is increased both by the frequency and by the amplitude of the motion.

As a result of the significant longitudinal induced velocities, measurements of the apparent vortex centre positions on the present photographs lead to over estimation of the lateral spacing. However, for the case shown in figure 1 it is

estimated that the error is no more than 4 % of the nominal value. This is in-significant compared with the scatter caused by flow irregularities. Because of this scatter it is difficult to detect any significant trend in the lateral spacing (figure 3). The only fact which emerges clearly is that the vortices are often spaced
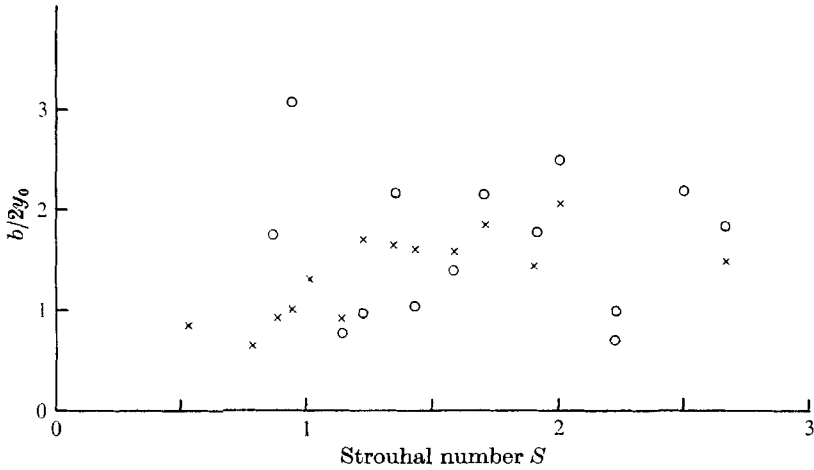

FIGURE 3. Comparison between lateral spacing b and displacement amplitude $2y_0$.
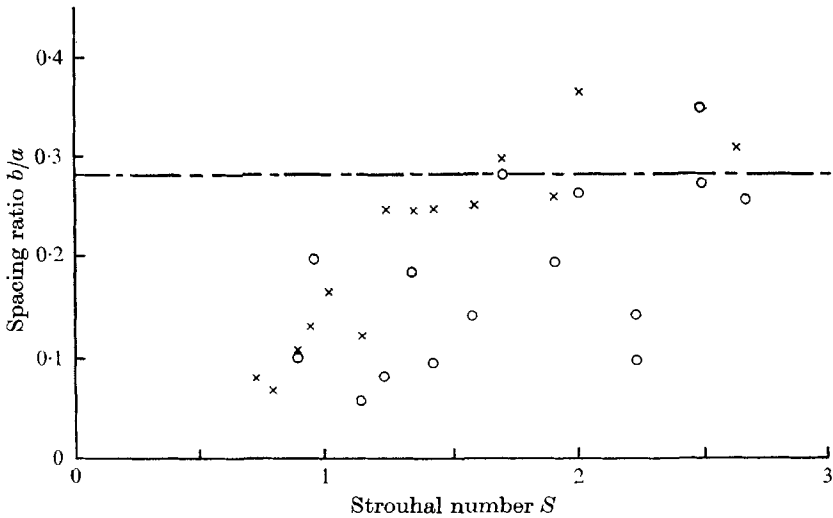$\times$, $y_0/c = 0.067$; $\bigcirc$, $y_0/c = 0.033$.

FIGURE 4. Variation of vortex spacing ratio with frequency.
$\times$, $y_0/c = 0.067$; $\bigcirc$, $y_0/c = 0.033$; —·—, von Kármán ratio 0.281.

well outside the limits of travel of the trailing edge. This point was examined further by means of some sequential sets of photographs, taken with a 35 mm automatic recording camera at 2–3 frames per second. These showed that not only does each vortex lie outside the aerofoil centreline when forming but also after separation it moves still further out under the influence of the cross-flow from the previous vortex.

When described in terms of the conventional spacing ratio b/a (figure 4) it is clear that many of the vortex trails differ considerably from the theoretically stable von Kármán pattern ($b/a = 0.281$). The experimental spacing ratio tends to increase with frequency and there is strong evidence of instability at the higher frequencies (figure 5, plate 1). Naturally, figure 4 contains very few points corresponding to this situation. At low frequencies, where the vortex trail is narrower than the von Kármán street, the wake is more stable.

Regular shedding at the oscillation frequency ceases only when replaced by the natural, high frequency drag type shedding which occurs in steady motion (figure 6, plate 1). This reversion from artificial to natural shedding corresponds to the termination of the 'locking in' phenomenon of Koopmann (1967) or to the 'hysteresis effect' of Bishop & Hassan (1963). In the present case, however, the reversion also includes a change from thrust type to drag type shedding.

An investigation is currently in progress at Oxford, which aims to provide more detailed information concerning the amplitudes and frequencies at which this sudden change takes place.

Comparison with unsteady aerofoil theory

It is well known that classical unsteady aerofoil theory does not recognize the formation of vortex trails. The normal assumption (Robinson & Laurmann 1956) is that the path of the aerofoil remains very close to a straight line and that any wake circulation is distributed along that line with no lateral displacement. It is not clear, however, to what extent the application of this theory is limited as amplitudes and frequencies increase. The onset of forced vortex shedding at relatively moderate amplitudes creates a wake so different from the assumed physical model that some doubt is cast upon the reliability of the more basic predictions of bound circulation, lift and pitching moment. The present experiments do not include force measurements,[†] but in the following section a comparison based upon wake circulation measurements is made in order to gain at least some indication of the limitations of the theory.

The theoretical circulation about an aerofoil in unsteady motion is given by Robinson & Laurmann (1956) in the general form

$$\Gamma = \pi c \exp(at - \tfrac{1}{2}\mu)(B_0 + B_1)/\mu(K_1(\tfrac{1}{2}\mu) + K_0(\tfrac{1}{2}\mu)). \tag{1}$$

In this equation, Γ is the instantaneous circulation about an aerofoil of chord c moving with constant forward velocity U and having a normal velocity component v given by

$$v = \left(\tfrac{1}{2}B_0 + \sum_{n=1}^{\infty} B_n \cos n\theta\right)\exp(at). \tag{2}$$

In these expressions $\mu = ac/U$ where a may be complex and K_0, K_1 are modified Bessel functions of the second kind.

[†] Successful dynamic force measurements on cylinders have been made directly by Bishop & Hassan (1963) and by Okajima & Asanuma (1969). In addition, Ferguson & Parkinson (1967) have measured oscillatory surface pressure distributions.

In the general form v depends not only upon time t but also on a chordwise position parameter θ. In the case of pure sinusoidal heaving motion, however, $a = i\omega$ and (2) becomes simply

$$v = v_0 \exp(i\omega t),$$

where v_0 ($=\frac{1}{2}B_0$) is the normal velocity amplitude and v_0/U is the incidence amplitude.

S	α	$\beta - \frac{1}{2}\nu$ (degrees)
0	1·0000	0
0·0064	0·9658	− 5·60
0·0191	0·8978	− 12·36
0·0637	0·7195	− 24·27
0·1591	0·5125	− 33·45
0·3183	0·3896	− 38·44
0·4775	0·3219	− 40·44
0·6366	0·2801	− 41·52
0·7958	0·2511	− 42·19
0·9549	0·2296	− 42·64
1·1141	0·2127	− 42·94
1·2732	0·1991	− 43·22
1·4324	0·1878	− 43·42
1·5916	0·1782	− 43·58
1·9099	0·1627	− 43·82
2·2282	0·1507	− 43·98
2·5465	0·1410	− 44·10
3·1831	0·1261	− 44·29

TABLE 1. Attenuation factor α and phase angle $\beta - \frac{1}{2}\nu$ from equation (3)

By the method of Robinson & Laurmann, (1) may then be reduced to

$$\Gamma/Uc = 2\pi(v_0/U)\exp i(\omega t - \tfrac{1}{2}\nu)/\tfrac{1}{2}\pi\nu((J_0(\tfrac{1}{2}\nu) - Y_1(\tfrac{1}{2}\nu)) - i(J_1(\tfrac{1}{2}\nu) + Y_0(\tfrac{1}{2}\nu))),$$

where J_n, Y_n are Bessel functions of the first and second kind respectively and $\nu = \omega c/U$. A more convenient form of this result is

$$\left.\begin{aligned}
& \Gamma/Uc = \alpha\pi(v_0/U)\exp i(\omega t - \tfrac{1}{2}\nu + \beta), \\
\text{where} \quad & 1/\alpha = \tfrac{1}{4}\pi\nu\{(J_0(\tfrac{1}{2}\nu) - Y_1(\tfrac{1}{2}\nu))^2 + (J_1(\tfrac{1}{2}\nu) + Y_0(\tfrac{1}{2}\nu))^2\}^{\frac{1}{2}}, \\
\text{and} \quad & \tan\beta = (J_1(\tfrac{1}{2}\nu) + Y_0(\tfrac{1}{2}\nu))/(J_0(\tfrac{1}{2}\nu) - Y_1(\tfrac{1}{2}\nu)).
\end{aligned}\right\} \quad (3)$$

Table 1 shows that the attenuation factor α approaches unity at zero frequency and the circulation then has the value $\pi v_0/U$ which corresponds to the steady flow case of an uncambered aerofoil at incidence v_0/U. In this limiting case the circulation is also in phase with the incidence since the phase lag angle $\frac{1}{2}\nu - \beta$ approaches zero.

As the frequency increases, however, the dimensionless circulation decreases rapidly and there is a phase lag which increases asymptotically to 45 degrees.

The periodic changes in bound circulation lead to a corresponding discharge of circulation from the trailing edge. Under the small amplitude assumption,

this circulation has no self-induced streamwise motion. Therefore the spatial distribution of circulation per unit length $\gamma(x)$ in the wake is given by

$$\gamma(x) = -\frac{1}{U}\frac{d\Gamma}{dt}. \tag{4}$$

Thus, using (3) we have

$$\gamma(x)/U = -\alpha\pi v_0 i\omega c\exp i(\omega t - \tfrac{1}{2}\nu+\beta)/U^2.$$

This may be expressed in terms of the amplitude y_0 and the wavelength λ of the aerofoil motion by writing $\omega\lambda = 2\pi U$, $Ut = x$, $v_0 = y_0\omega$ so that

$$\gamma(x)\lambda^2/Ucy_0 = 4\pi^3\alpha\exp i(2\pi x/\lambda - \tfrac{1}{2}\pi - \tfrac{1}{2}\nu+\beta)\ldots \tag{5}$$

Ideal vortex strength

The physical significance of (5) is made clearer if it is remembered that, despite the assumptions of the theory, the trailing edge of the aerofoil traces a sinusoidal path in space described by

$$y = y_0\exp i(2\pi x/\lambda - \tfrac{1}{2}\pi). \tag{6}$$

Thus, if it is assumed that instead of being distributed along the mean path $y = 0$ the wake circulation is deposited initially along the actual path of the trailing edge, then this deposition of circulation is sinusoidal not only in magnitude (equation (5)) but also in position (equation (6)). Between these two variations there is a phase lag $\tfrac{1}{2}\nu - \beta$ which will be discussed later.

Now it has been shown by Olmstead (private communication) that in an isolated infinite array, this type of circulation distribution tends to roll up into discrete vortices. These are indications that, in the limit, each vortex would contain all the vorticity of one sign shed in each half cycle. Thus it is to be expected that the ideal or maximum possible strength of any discrete wake vortice will be equal to the peak-to-peak change in the aerofoil circulation. This value, Γ_i is obtained by inspection of (3)

$$\Gamma_i/Uc = 2\pi\alpha v_0/U,$$

or in the notation of (5) and (6)

$$\Gamma_i\lambda/Ucy_0 = 4\pi^2\alpha. \tag{7}$$

Clearly, while weaker vortices than this may be shed by a phase alteration which causes mixing of positive and negative vorticity, it is quite impossible to generate a stronger vortex without increasing the bound circulation amplitude. Γ_i is therefore the theoretical maximum vortex strength.

Vortex strength measurements

This expression is plotted in figure 7, together with the measured vortex strength from the present experiments. The circulation about each vortex was found by integrating the tangential velocity components round a suitable circle (Wood 1967, 1968). Each point in figure 7 represents the average strength of the three or four most recently formed vortices in one photograph.

The dimensionless vortex strength parameter $\Gamma\lambda/Ucy_0$ suggested by (7) gives a good collapse of the experimental data for amplitudes which vary over an order of magnitude ($y_0/c = 0.08$ down to 0.008). However, the quantitative agreement with the theoretical curve deteriorates as the Strouhal number increases.
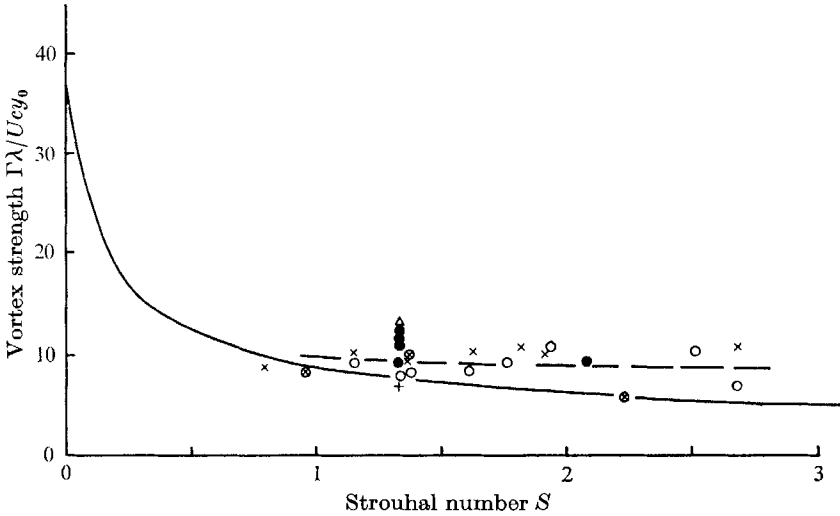

FIGURE 7. Variation of vortex strength with frequency. $\triangle$, $y_0/c = 0.0083$; $+$, $y_0/c = 0.0167$; $\bigcirc$, $y_0/c = 0.033$; $\times$, $y_0/c = 0.067$; $\bullet$, $y_0/c = 0.083$; ——, equation (7) with table 1; — —, experiment.

In discussing this discrepancy it must be noticed that for a given amplitude y_0/c of the sinusoidal motion, the maximum inclination of the aerofoil path increases with frequency so that the incidence amplitude is $2\pi Sy_0/c$. For a typical experimental amplitude $y_0/c = 0.033$ (figure 7) an incidence amplitude of 10 degrees is reached at $S = 0.835$. The minimum inclination for which the shedding was strong enough to be represented in figure 7, appears at $S = 1.34$, $y_0/c = 0.0083$ and is no more than 4 degrees.

It is significant, therefore, that below $S = 1$ not only do the theoretical and experimental curves begin to agree quite well, but also the vortex trails tend to become too weak to measure. In this result there is a clear indication that the validity of the small amplitude assumption is limited by the onset of strong vortex shedding and that this limit may be described in terms of a reasonable incidence restriction.

At higher Strouhal numbers, the average trend of the present experimental points indicates that the wake vortices become up to 50% stronger than the maximum possible value indicated by the theory. This comparison leads to the conclusion that the presence of a vortex trail must increase the amplitude of the bound circulation by this factor.

Under conditions of wake vortex generation, therefore, the classical theory (Robinson & Laurmann 1956) appears to be inadequate for the prediction of

bound circulation. To a certain extent, this conclusion also casts suspicion upon the theoretical results for lift and pitching moment.

However, the present experiments do not give sufficient evidence to support a firm conclusion here. In unsteady flow the forces do not depend upon circulation alone, but also upon additional inertia terms which become dominant as the frequency increases.

Phase observations

Equations (5) and (6) suggest that between the theoretical strength of the wake vortex sheet and its lateral displacement there is a frequency dependent phase difference $\beta - \frac{1}{2}\nu$. Now by sign convention (Robinson & Laurmann 1956) anti-clockwise circulation is positive and the aerofoil moves from right to left. Therefore at low frequency, when $\beta - \frac{1}{2}\nu$ approaches zero (table 1) the two waves are in phase so that maximum anticlockwise circulation coincides with maximum upward displacement and *vice versa*. At higher frequencies the maximum circulation is shed later and is positioned up to 45 degrees in phase closer to the aerofoil than the peak displacement. Table 1 shows that over the present experimental frequency range the theoretical phase lag remains close to 45 degrees. This suggests that when discrete vortices are shed, they may not appear at the maximum displacement positions of the trailing edge but could form later as the aerofoil moves inwards.

In order to study this aspect of the flow, an electrically operated 35 mm automatic recording camera (Robot) was triggered from a photo-electric cell. The light to this cell was interrupted by a projecting flag on the driving crank wheel of the oscillating mechanism. Thus by positioning the flag at 10 degree intervals round the crank wheel and allowing for the shutter time lag, photo-graphs could be taken at known stages of the oscillation cycle. It is estimated that at the mid-point of the 33 ms exposure, the crank position was known within 3·6 degrees (r.m.s.) at the highest frequency used.

The resulting series of photographs show that each vortex develops slowly as vorticity is fed directly into it from the trailing edge (figure 8 (*a*) and (*b*), plate 2).

At Strouhal numbers between 0·7 and 2·7, most of the growth took place between 30 degrees and 80 degrees after the displacement peak. This confirms the existence of a substantial phase lag in the predicted sense although it does not give an accurate indication of the magnitude.

Although most of the growth took place within the angle range just mentioned, a few photographs showed that even as late as 108 degrees, the vortex still had not separated completely from the trailing edge. At the other extreme, some slight indication of an incipient vortex was observed only 18 degrees after the displacement peak. Figures 8 (*a*) and (*b*) show the development at 46 and 96 degrees respectively. Theoretically, of course, a sinusoidal variation in bound circulation with a 45 degree phase lag would cause the vortex growth to commence 45 degrees before the displacement peak and to last for exactly half a cycle. Conversely, any gap between the separation of one vortex and the initiation of the next must imply that the waveform is not sinusoidal but is of a plateau type in which the peak value is maintained for a finite interval.

The information gained from the present experiments is not sufficient to suggest a firm conclusion on this question. It can only be suggested that the circulation wave form is probably smooth but it is unlikely to be sinusoidal.

4. Results: Jet flap aerofoil

The theory of aerofoil in unsteady motion has been extended by Spence (1965) to include the case of a jet flap. Spence's theory depends upon the usual small displacement assumption and the results were expressed in terms of a dimensionless frequency parameter denoted here by the symbol n, where

$$n = \pi(h/c)(V\gamma/U)^2 S.$$

In this expression h is the width of the jet slit and V_y/U is the jet-to-stream velocity ratio.

One of the features of the theoretical analysis was the absence of a solution for $n > 2$. Therefore the present experiments were planned initially to see whether any unusual feature could be observed under these conditions.

The experiments were basically similar to those described in §3. The model had been designed to produce an undeflected jet sheet through a slit 2·06 mm wide in the trailing edge. Uniform flow distribution in the jet was obtained by drilling the brass manifold with an array of holes according to the one-dimensional manifold theory of Horlock (1956), Wood (1967). The drilled portion of the tube wall was specially thickened by the addition of a 7 mm brass strip so that the distribution holes would be longer and more effective in removing the axial velocity component from the internal flow. When tested by traversing a small pilot tube along the span, the jet velocity was found to be uniform within $\pm 10\%$. The internal flow was metered by a sharp edged orifice and was pumped to the trolley via an overhead swinging boom. Marker particles for photography could be used either in the jet or in the tank.

The motion was photographed mainly at $S = 1·35$ with V_y/U ranging from 0 to 10. Several forward velocities were used between 0·04 m/s ($Re_c = 0·5 \times 10^4$) and 0·13 m/s ($Re_c = 1·8 \times 10^4$). In this way, values of n were obtained up to 5·7 but at no point were there any distinctive flow features which might have been related to the failure of the Spence solution.

As in the case of the plain aerofoil, the fundamental difference between the observed flow and the theoretical model was the generation of a vortex trail (figure 9, plate 2). In each case the jet sheet was drawn into the vortices and did not converge on to the mean path as predicted by Spence.

The effect of the jet was to increase both the strength and the spacing of the vortices when compared with the jet off case (figures 10 to 12). The infinite street momentum equation

$$T = lU\Gamma b/a + \Gamma^2 l\{2\pi(b/a)\tanh(\pi b/a) - 1\}/2a\pi$$

(which is derived by changing the sign of Γ in the classical expression (Goldstein 1938; Michelson 1963)), suggests that the increases in Γ and b/a both

correspond to an increase in thrust. This effect therefore is quite compatible with the absorption of the jet momentum into the wake.

At first sight the prospect of a comparison between the measured vortex strength and a theoretical estimate of the aerofoil circulation (cf. figure 7)
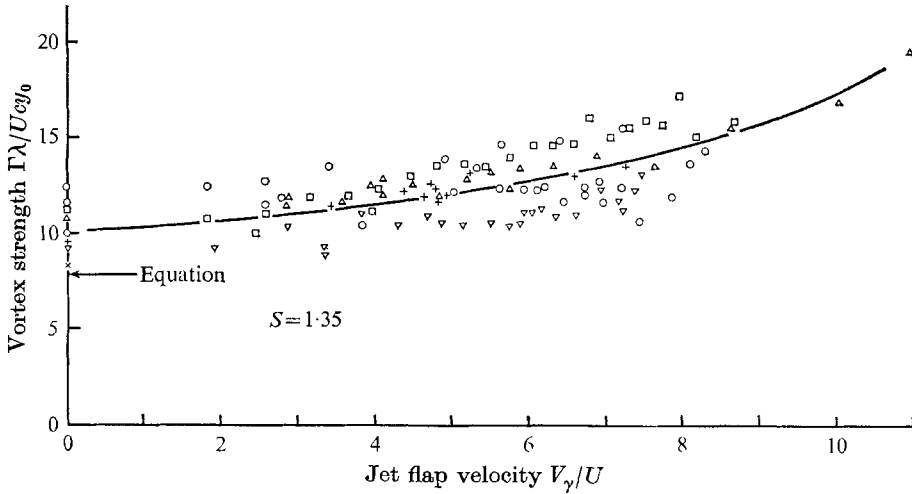

FIGURE 10. Variation of vortex strength with jet flap velocity.
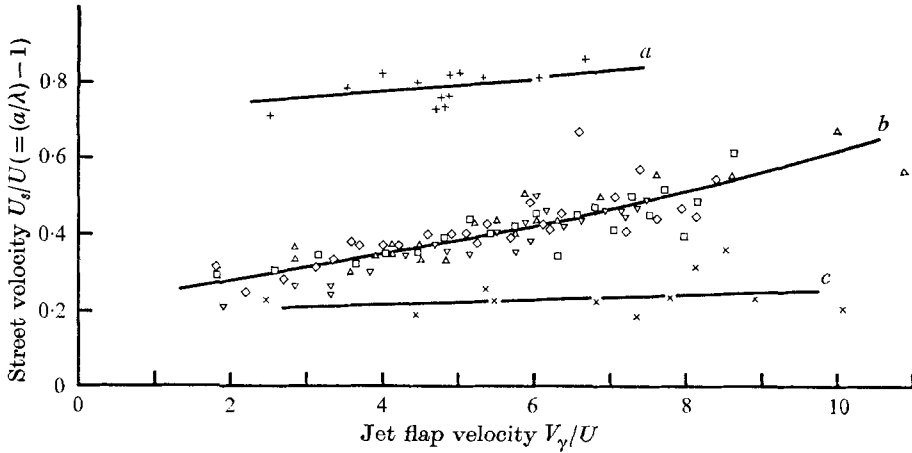See table 2 for definition of the symbols.

FIGURE 11. Variation of longitudinal vortex spacing with jet flap velocity. a, $S = 2.08$, $y/c = 0.08$; b, $S = 1.35$, $y/c = 0.08$; c, $S = 1.35$, $y/c = 0.03$. See table 2 for definition of the symbols.

seems inviting. However, in this case, such a comparison would be meaningless because of the circulation contribution made by the jet sheet itself in the down-wash equation (Spence 1965). Although the jet is recognizable only for a very small distance in the present case, this effect must still exist so that the aerofoil circulation is not the only factor which influences the vortex strength.
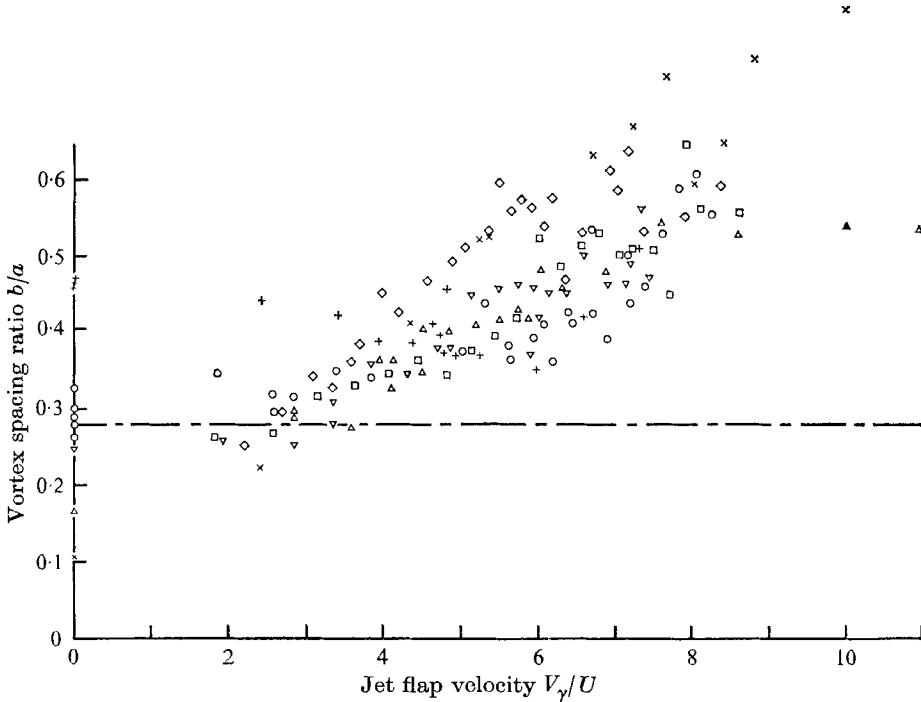
FIGURE 12. Variation of vortex spacing ratio with jet flap velocity. —·—, von Kármán spacing 0·281. See table 2 for definition of symbols.

	S	y_0/c	Re_c
○	1·35	0·125	$1·245 \times 10^4$
□	1·35	0·08	$1·24 \times 10^4$
◇	1·35	0·08	$1·79 \times 10^4$
▽	1·35	0·08	$0·83 \times 10^4$
△	1·35	0·08	$0·50 \times 10^4$
+	2·08	0·08	$0·83 \times 10^4$
×	1·35	0·03	$1·24 \times 10^4$

TABLE 2. Key to symbols used in figures 10, 11 and 12

5. Conclusion

Flow visualization tests at chord Reynolds numbers of order 10^4 have shown that distinct vortex trails are generated by heaving aerofoils when the wavelength of the motion becomes less than the aerofoil chord ($S \geqslant 1$). This is true for amplitudes greater than about 3 % of the chord, but vortex generation has been observed at slightly higher frequencies for dimensionless amplitudes (y_0/c) as low as 0·008.

The agreement between the measured vortex strength and the values deduced from the results of thin aerofoil theory deteriorates as the shedding becomes stronger until at $S > 2$ the average strength of the wake vortices is 50 % greater

than the theoretical peak-to-peak circulation change. It is concluded therefore that thin aerofoil theory underestimates the circulation amplitude and possibly also the lift amplitude in vortex shedding situations.

Had this discrepancy been of opposite sign, then there would have been the possibility of a loss of circulation, similar perhaps to that which puzzled the early investigators of the bluff body shedding problem (e.g. Fage & Johansen 1928). However, this is not the case and therefore the present results constitute a certain confirmation of the validity of the conservation type of assumption (see equation (4)) which is used to relate the vortex street to the variations in bound circulation. A further confirmation is given by the phase relationship between the shedding and the motion. As far as could be observed, this is of similar order to the 45 degree lag predicted by the theory.

Because the frequency and the amplitude are controlled separately, vortex trails are generated which differ considerably in some cases from the theoretically stable von Kármán pattern ($b/a = 0.281$). These are violently unstable and persist only for a very short time when $b/a > 0.281$ but seem to be relatively stable in the narrower configurations. The final disruption of the controlled frequency shedding at small amplitudes occurs when the weak shedding pattern is overcome suddenly by a high frequency drag type of shedding.

The presence of a jet flap does not suppress the vortex shedding but rather amplifies it. The thrust effect of the flapping motion is supplemented by the absorption of the jet momentum into the vortex trail and the strength and spacing of the vortices is increased.

No conclusion can be drawn from the present experiments concerning the effect of vortex shedding on the oscillatory lift force whose magnitude is predicted by Spence. However, the wake flow does differ strikingly from the predicted jet configuration. Furthermore, there is no evidence of any change in the nature of the flow which might be associated with the failure of the theoretical solution for $n > 2$.

REFERENCES

BISHOP, R. & HASSAN, A. Y. 1963 *Proc. Roy. Soc.* A **277**, 32–51.

FAGE, A. & JOHANSEN, F. C. 1928 *Aero. Res. Coun. R & M* **1143**, 558–562.

FERGUSON, N. & PARKINSON, G. V. 1967 *Trans. Am. Soc. Mech. Engrs.* B **89**, 831–838.

GOLDSTEIN, S. 1938 *Modern Developments in Fluid Dynamics*. Oxford University Press.

HORLOCK, J. H. 1956 *J. Roy. Aero. Soc.* **60**, 749–752.

KOOPMANN, G. H. 1967 *J. Fluid Mech.* **28**, 501–512.

MICHELSON, I. 1963 *J. Am. Inst. Aero. Astro.* **1**, 2658.

OKAJIMA, A. & ASANUMA, T. 1969 Unpublished report.

PARKER, R. 1966a *J. Sound Vib.* **4**, 62–72.

PARKER, R. 1966b *J. Sound Vib.* **5**, 330–343.

PARKER, R. 1967a *J. Sound Vib.* **6**, 302–309.

PARKER, R. 1967b *J. Sound Vib.* **7**, 371–379.

ROBINSON, A. & LAURMANN, J. A. 1956 *Wing Theory.* Cambridge University Press.

SPENCE, D. A. 1965 *Phil. Trans. Roy. Soc.* A **257**, 445–473.

TOEBES, G. H. & EAGLESON, P. S. 1961 *Am. Soc. Mech. Engng (J. Basic. Engng)*, 671–677.

WOOD, C. J. 1967 *J. Fluid Mech.* **29**, 259–272.
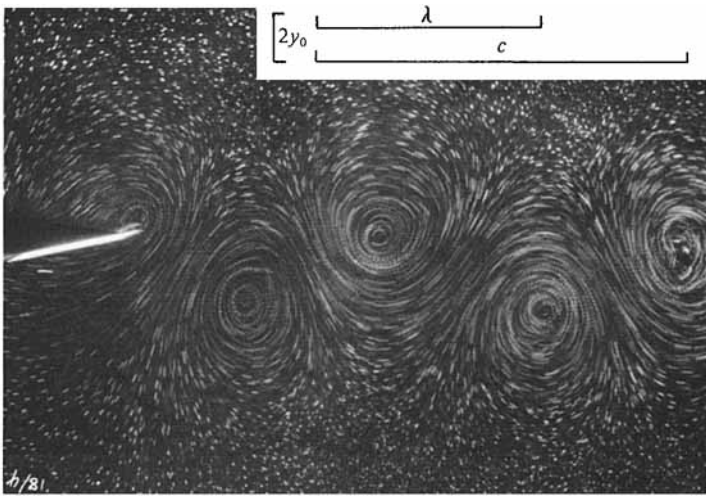
WOOD, C. J. 1968 *J. Sci. Inst.* **2**, 475.

FIGURE 1. Typical vortex trail from heaving aerofoil. $y_0/c = 0.067, S = 1.625$.
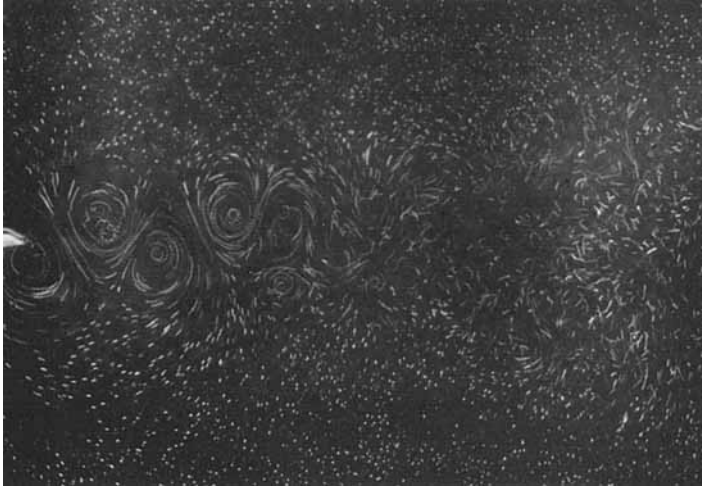
FIGURE 5. Unstable vortex trail. $y_0/c = 0.033$; $S = 3.15$.
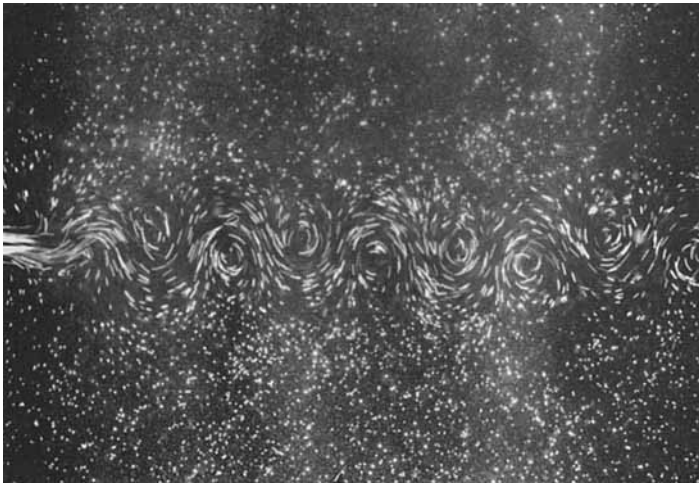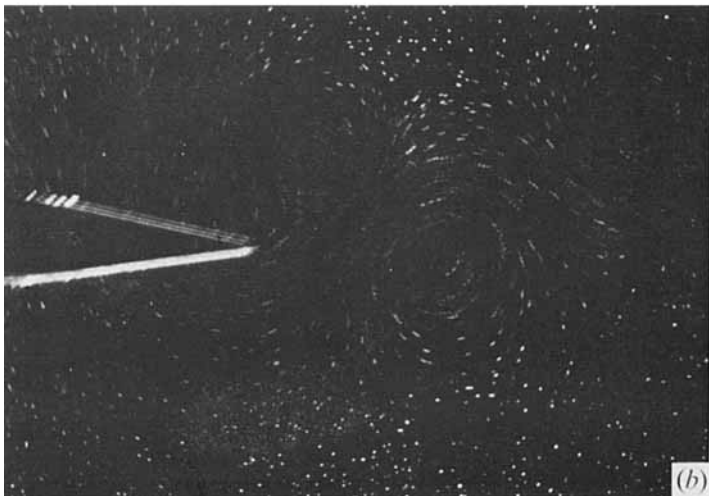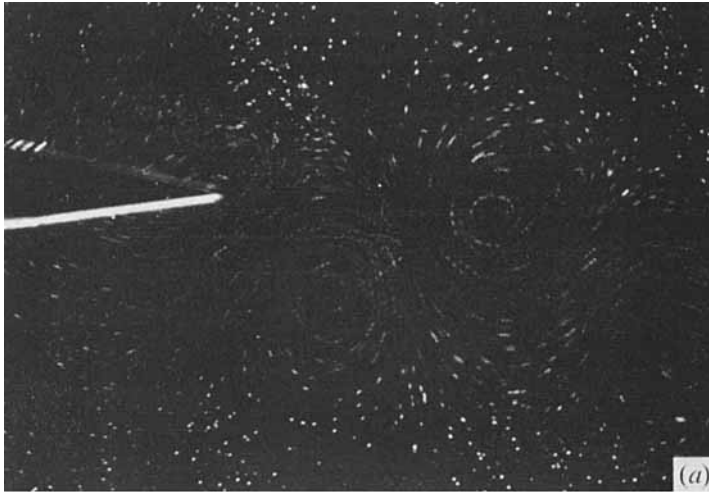

FIGURE 6. Vortex trail with no oscillation.

FIGURE 8. Vortex growth. (a) 18° A.T.D.C., (b) 108° A.T.D.C.
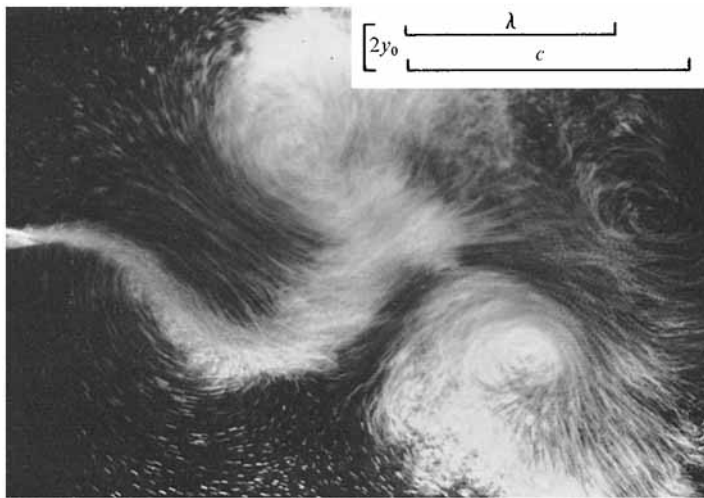
FIGURE 9. Heaving jet flap. $y_0/c = 0.083$, $S = 1.33$, $V_\gamma/U = 6.60$, $n = 2.42$.